POWER FLOW IN COMPLEX FORM BASED LOADABILITY ASSESSMENT

[1]PhD Iu. Axente, PhD, prof. I. [2]Stratan
University of Western Ontario, London, Technical University of Moldova

INTRODUCTION

There was a time when electric utilities could afford building oversized transmission systems. However, this state of affairs has appreciably changed as a result of power system restructuring and deregulation. Nowadays, working under economical and environmental constraints, utilities rarely resort to transmission system expansion. Due to this and some other factors, in the last three decades, transmission systems have been operated much closer to their voltage stability limit (or loadability limit). Several factors are responsible for this [1]: environmental pressures on transmission expansion, increased electricity consumption in heavy load areas (where it is not feasible or economical to install new generating plants), new system loading patterns due to the opening up of the electricity market, etc. A number of voltage instability incidents have been experienced around the world [2]. As a consequence, voltage stability has become a major concern in power system planning and operation. From the power system security point of view, knowledge of the critical power and voltage is very important as the operating voltage, and power, at the system nodes should be kept as far away as possible from their critical values. Online monitoring of the stability status is essential when operating the system near its loadability limit. As expected, significant research efforts have been devoted to construct a more comprehensive understanding of voltage stability issues and develop methods for recognizing and resolving them.

Various loadability assessment methods have been proposed in the literature [1]-[16], most of them being suitable only for offline system analysis. Usually these methods are based on power flow analysis and properties of the associated Jacobian matrix. However, in a real power system, the size of the problem is so large that the computation is too time-consuming; therefore most of these methods are unsuitable for online loadability assessment. Perhaps the simplest loadability assessment method is to repeatedly perform power flow computations, gradually increasing the load until the loadability limit is slightly violated and convergence to any real solution is no longer possible. However, this method has an inherent convergence problem in close proximity of loadability limit point because the power flow Jacobian matrix becomes singular at this point. The continuation power flow method [1]-[6] overcomes this problem by reformulating the power flow equations so that they remain well-conditioned at all possible loading conditions. Although the continuation method is robust and flexible, it is very slow and time-consuming. A method based on continuation power flow using model trees is proposed in [7], which has an increased computation speed. In [8]-[12] and [24], the problem of maximum loadability limit determination is formulated as an optimization problem. The latter paper proposes a direct internal point optimization method, which is very effective in dealing with a great number of power flow unsolvable cases, when the Jacobian matrix is ill-conditioned. Neural networks based approaches for online prediction of the closest loadability margin are proposed in [13]-[14]. Another approach for real-time determination of loadability limit, successfully installed and proven in several Energy Management Systems, is presented in [15]. An approach for maximum loadability assessment in a probabilistic framework is proposed in [16].

In this paper, a new approach for loadability assessment is proposed, which is based on power flow in complex form. It is well-known [20] (page 98) that the complex power flow equations do not meet Cauchy-Riemann conditions [21] (page 35); therefore the Newton-Raphson method cannot be directly applied in this case. Conventionally, this problem is overcome by splitting each complex power flow equation into two real equations. The approach proposed in this paper consists in performing some manipulations on conventional complex power flow equations and as a result obtaining a new system of complex power flow equations, which meet Cauchy-Riemann conditions. Thus, now the calculation of derivatives with respect to complex variables is possible, consequently the Newton-Raphson method can be directly applied to complex power flow equations. Moreover, these new complex power flow equations have solutions beyond the loadability limit

point, which can be successfully employed in loadability assessment. An approach for solving the power flow equations in complex form has been previously reported in [17]-[19], but it involves solving twice as many complex power flow equations as usual and has some significant drawbacks discussed in section V.

Also, this paper proposes a new approach for loadability assessment, named parabola approximation approach, which is based on some properties of the solutions obtained beyond the loadability limit point. It consists in performing three computations of power flow in complex form beyond the loadability limit point, and then based on obtained solutions the imaginary part of PV curve is approximated by a parabola the constant term of which is the node power limit. Since only three power flow computations have to be performed, the proposed approach is not much time-consuming and can be successfully applied in online loadability assessment.

1.POWER FLOW IN COMPLEX FORM

First, the concept of Power Flow in Complex Form is explained using a two-node system. Then, its application to a multi-node system is presented.

A. Two-node System

For a two-node system, it is possible to analytically obtain the power flow solutions and determine the loadability limit. Therefore, the two-node system analysis presented below will be useful for gaining insight into the proposed concepts.

The power flow computation for a two-node system shown in Figure 1 involves solving the following equation:

$$\left(\overline{Y}_{11}\overline{U}_1+\overline{Y}_{12}\overline{U}_2\right)\hat{U}_1=\hat{S}_1 \tag{1}$$

Alternatively, the following equation, which is the conjugate of (1), can be solved:

$$\left(\hat{Y}_{11}\hat{U}_1+\hat{Y}_{12}\hat{U}_2\right)\overline{U}_1=\overline{S}_1 \tag{2}$$

The well known Newton-Raphson technique cannot be directly applied to solve (1), because it does not satisfy the Cauchy–Riemann conditions [21] (page 35), hence preventing the application of derivatives in complex form [20] (page 98). Therefore, the conventional way of solving (1) is to split it into two real equations and solve them simultaneously applying the Newton-Raphson method. It is well known that (1) has no solutions beyond the loadability limit point, therefore the conventional power flow diverges. Also, the Newton-Raphson technique is prone to divergence in the proximity of loadability limit point (because of singularity of the Jacobian matrix), although solutions exist. Thus, sometimes it is not clear whether the divergence is caused by system overloading or it is due to imperfections of the solution technique used in power flow computation.

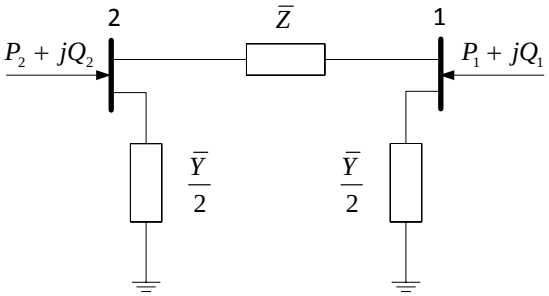

Figure 1. Two-node power system.

In order to be able to apply the Newton-Raphson method in complex form the following approach is proposed.

From (2), the expression for calculating $\hat{U}_1$ is obtained:

$$\hat{U}_1=-\frac{\hat{Y}_{12}}{\hat{Y}_{11}}\hat{U}_2+\frac{1}{\hat{Y}_{11}}\frac{\overline{S}_1}{\overline{U}_1} \tag{3}$$

Now, after substituting (3) in (1)(1) and performing some manipulations, the following quadratic equation is obtained:

$$\overline{A}\,\overline{U}_1^2+\overline{B}\,\overline{U}_1+\overline{C}=0 \tag{4}$$

Where: $\overline{A}=-\overline{Y}_{11}\hat{Y}_{12}\hat{U}_2$,

$$\overline{B}=\overline{Y}_{11}\overline{S}_1-\hat{Y}_{11}\hat{S}_1-\overline{Y}_{12}\hat{Y}_{12}\overline{U}_2\hat{U}_2,$$

$$\overline{C}=\overline{Y}_{12}\overline{U}_2\overline{S}_1.$$

Equation (4) has the following properties which have been identified through analytical and numerical investigations:

1) It satisfies the Cauchy–Riemann conditions, so the Newton-Raphson method in complex form can be applied for solving it.

2) Its discriminant is a real number, which is positive up to the loadability limit point and negative beyond it.

3) It has two solutions, both up to and beyond the loadability limit point.

4) Up to the loadability limit, one of the solutions corresponds to the stable steady-state (upper part of PV-curve) and the other one to the unstable steady-

state (lower part of PV-curve).

5) In the point of loadability limit the discriminant is equal to zero and there is only one solution.

6) Solutions obtained up to the loadability limit point satisfy (1) and (2).

7) A solution obtained up to the loadability limit being substituted in (3) will result in its conjugate.

8) Solutions obtained beyond the loadability limit point mathematically satisfy the applied model (equation (4)), but they cannot physically exist in a real power system.

9) Any solution obtained beyond the loadability limit point being substituted in (3) will not result in its conjugate. Thus, beyond the loadability limit point $\hat{U}_1$ calculated with (3) is not equal to the conjugate of $\overline{U}_1$ and this fact can serve as criterion that the power enforced in node 1 is above the loadability limit.

The voltage magnitude in node 1 V_1 can be calculated with the following formula:

$$V_1 = \sqrt{\overline{U}_1 \hat{U}_1} \qquad (5)$$

Since up to the loadability limit point $\hat{U}_1$ is equal to the conjugate of $\overline{U}_1$, V_1 is a real number. As mentioned above, beyond the loadability limit point, $\hat{U}_1$ (calculated with (3)) is not equal to the conjugate of $\overline{U}_1$, therefore in this case V_1 is a complex number. Thus, beyond the loadability limit point, V_1 has the imaginary part and the two solutions obtained for V_1 are complex conjugates. These two solutions obtained beyond the loadability limit point mathematically satisfy the applied model, but they cannot physically exist in a real power system. However, the fact that V_1 calculated with (5) is a complex number indicates that the power enforced in node 1 is above the loadability limit.

Now, let us exemplify, considering a two-node system with the following parameters:

$\overline{Z} = 24.48 + j34.72\ \Omega$, $\overline{Y} = j208.8 \cdot 10^{-6}$ S, $\overline{U}_2 = 116$ V.

For a two-node system, the power limit can be calculated analytically, by equating the discriminant of (4) to zero and solving the resulting equation for P_1, provided that $\cos\theta_1$ (power factor) is known. In the two-node system under consideration, assuming that $\cos\theta_1 = 0.85$ (lagging), the analytically calculated power limit in node 1 is: $P_{1,\lim} = -70.31848097515315$ MW.

Stressing the system by gradually increasing the consumption in node 1 from 0 to 100 MW (in steps of 0.1MW),while keeping $\cos\theta_1 = const = 0.85$ (lagging), a series of solutions for V_1 has been obtained. Using these solutions the PV curve shown in Figure 2 has been drawn.

From Figure 2 we can see that up to the loadability limit point the voltage magnitude in node 1 V_1 is a real number (the imaginary part is zero). Beyond the loadability limit point V_1 is a complex number (the imaginary part is different from zero). Also, the two solutions obtained for V_1 are complex conjugates.

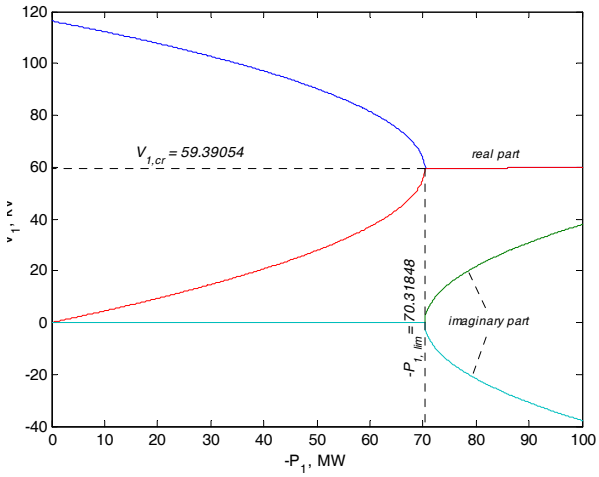

Figure 2. PV curve for the two-node system under consideration.

B. Multi-node System

The idea explained in previous subsection for a two-node system is equally applicable to a multi-node power system. For convenience and ease of explanation the system nodes are numbered as follows:

N_{PQ} – number of *PQ*-nodes;
N_{PV} – number of *PV*-nodes;
$N = N_{PQ}+N_{PV}+1$ – total number of nodes;
$1 \ldots N_{PQ}$ – *PQ*-nodes;
$N_{PQ}+1 \ldots N_{PQ}+N_{PV}$ – *PV*-nodes;
N – *Slack*-node.

For each PQ-node ($i = 1 \ldots N_{PQ}$) the following equation is written:

$$\hat{U}_i \sum_{k=1}^{N} \overline{Y}_{i,k} \overline{U}_k = \hat{S}_i \qquad (6)$$

For each PV-node ($i = N_{PQ}+1 \ldots N_{PQ}+N_{PV}$) the following equation is written:

$$\hat{U}_i \sum_{k=1}^{N} \overline{Y}_{i,k}\, \overline{U}_k + \overline{U}_i \sum_{m=1}^{N} \hat{Y}_{i,m}\, \hat{U}_m = 2\, P_i \tag{7}$$

Also, for each PQ-node ($i = 1 \ldots N_{PQ}$) the following equation is written:

$$\sum_{k=1}^{N} \hat{Y}_{i,k}\, \hat{U}_k = \frac{\overline{S}_i}{\overline{U}_i} \tag{8}$$

Finally, for each PV-node ($i = N_{PQ}+1 \ldots N_{PQ}+N_{PV}$) the following equation is written:

$$\hat{U}_i = \frac{V_i^2}{\overline{U}_i} \tag{9}$$

Equations (8) and (9) combined together and presented in matrix form look as follows:

$$\begin{bmatrix} [\hat{Y}_{PQ}] & [\hat{Y}_{PV}] \\ [0] & [E] \end{bmatrix} \cdot \begin{bmatrix} [\hat{U}_{PQ}] \\ [\hat{U}_{PV}] \end{bmatrix} = \begin{bmatrix} [\overline{S}_d] & [0_1] \\ [0_2] & [V_d^2] \end{bmatrix} \cdot \begin{bmatrix} [\overline{U}_{PQ}^{-1}] \\ [\overline{U}_{PV}^{-1}] \end{bmatrix} - \begin{bmatrix} [\hat{I}_{slack}] \\ [0_3] \end{bmatrix} \tag{10}$$

Where:

Zero matrixes $[0]$, $[0_1]$, $[0_2]$, $[0_3]$ and identity matrix $[E]$ have the following sizes: $N_{PV} \times N_{PQ}$, $N_{PQ} \times N_{PV}$, $N_{PV} \times N_{PQ}$, $N_{PV} \times 1$ and $N_{PV} \times N_{PV}$, respectively.

$$[\hat{Y}_{PQ}] = \begin{bmatrix} \hat{Y}_{1,1} & \hat{Y}_{1,2} & \cdots & \hat{Y}_{1,N_{PQ}} \\ \hat{Y}_{2,1} & \hat{Y}_{2,2} & \cdots & \hat{Y}_{2,N_{PQ}} \\ \cdots & \cdots & \cdots & \cdots \\ \hat{Y}_{N_{PQ},1} & \hat{Y}_{N_{PQ},2} & \cdots & \hat{Y}_{N_{PQ},N_{PQ}} \end{bmatrix}$$

$$[\overline{S}_d] = \begin{bmatrix} \overline{S}_1 & 0 & \cdots & 0 \\ 0 & \overline{S}_2 & \cdots & 0 \\ \cdots & \cdots & \cdots & \cdots \\ 0 & 0 & \cdots & \overline{S}_{N_{PQ}} \end{bmatrix}$$

$$[\hat{Y}_{PV}] = \begin{bmatrix} \hat{Y}_{1,N_{PQ}+1} & \hat{Y}_{1,N_{PQ}+2} & \cdots & \hat{Y}_{1,N_{PQ}+N_{PV}} \\ \hat{Y}_{2,N_{PQ}+1} & \hat{Y}_{2,N_{PQ}+2} & \cdots & \hat{Y}_{2,N_{PQ}+N_{PV}} \\ \cdots & \cdots & \cdots & \cdots \\ \hat{Y}_{N_{PQ},N_{PQ}+1} & \hat{Y}_{N_{PQ},N_{PQ}+2} & \cdots & \hat{Y}_{N_{PQ},N_{PQ}+N_{PV}} \end{bmatrix}$$

$$[V_d^2] = \begin{bmatrix} V_{N_{PQ}+1}^2 & 0 & \cdots & 0 \\ 0 & V_{N_{PQ}+2}^2 & \cdots & 0 \\ \cdots & \cdots & \cdots & \cdots \\ 0 & 0 & \cdots & V_{N_{PQ}+N_{PV}}^2 \end{bmatrix}$$

$$[\hat{I}_{slack}] = \begin{bmatrix} \hat{Y}_{1,N} \\ \hat{Y}_{2,N} \\ \cdots \\ \hat{Y}_{N_{PQ},N} \end{bmatrix} \cdot \hat{U}_N$$

$$[\hat{U}_{PQ}] = \begin{bmatrix} \hat{U}_1 \\ \hat{U}_2 \\ \cdots \\ \hat{U}_{N_{PQ}} \end{bmatrix} \qquad [\hat{U}_{PV}] = \begin{bmatrix} \hat{U}_{N_{PQ}+1} \\ \hat{U}_{N_{PQ}+2} \\ \cdots \\ \hat{U}_{N_{PQ}+N_{PV}} \end{bmatrix} \qquad [\hat{U}] = \begin{bmatrix} [\hat{U}_{PQ}] \\ [\hat{U}_{PV}] \end{bmatrix}$$

$$[\overline{U}_{PQ}^{-1}] = \begin{bmatrix} 1/\overline{U}_1 \\ 1/\overline{U}_2 \\ \cdots \\ 1/\overline{U}_{N_{PQ}} \end{bmatrix} \qquad [\overline{U}_{PV}^{-1}] = \begin{bmatrix} 1/\overline{U}_{N_{PQ}+1} \\ 1/\overline{U}_{N_{PQ}+2} \\ \cdots \\ 1/\overline{U}_{N_{PQ}+N_{PV}} \end{bmatrix} \qquad [\overline{U}^{-1}] = \begin{bmatrix} [\overline{U}_{PQ}^{-1}] \\ [\overline{U}_{PV}^{-1}] \end{bmatrix}$$

The inverse of matrix $\begin{bmatrix} [\hat{Y}_{PQ}] & [\hat{Y}_{PV}] \\ [0] & [E] \end{bmatrix}$ is calculated as follows:

$$[\hat{Z}] = \begin{bmatrix} [\hat{Y}_{PQ}] & [\hat{Y}_{PV}] \\ [0] & [E] \end{bmatrix}^{-1} = \begin{bmatrix} [\hat{Z}_{PQ}] & [\hat{Z}_{PV}] \\ [0] & [E] \end{bmatrix} \tag{11}$$

Where: $[\hat{Z}_{PQ}] = [\hat{Y}_{PQ}]^{-1}$ and $[\hat{Z}_{PV}] = -[\hat{Y}_{PQ}]^{-1} \cdot [\hat{Y}_{PV}]$.

After the left multiplication of both sides of (10) by $[\hat{Z}]$ the following equation is obtained:

$$\begin{aligned} [\hat{U}] = \begin{bmatrix} [\hat{U}_{PQ}] \\ [\hat{U}_{PV}] \end{bmatrix} = \begin{bmatrix} [\hat{Z}_{PQ}] & [\hat{Z}_{PV}] \\ [0] & [E] \end{bmatrix} \cdot \\ \cdot \left(\begin{bmatrix} [\overline{S}_d] & [0_1] \\ [0_2] & [V_d^2] \end{bmatrix} \cdot \begin{bmatrix} [\overline{U}_{PQ}^{-1}] \\ [\overline{U}_{PV}^{-1}] \end{bmatrix} - \begin{bmatrix} [\hat{I}_{slack}] \\ [0_3] \end{bmatrix} \right) \end{aligned} \tag{12}$$

Now, the following notations are introduced:

$$[\overline{A}] = \begin{bmatrix} [\hat{Z}_{PQ}] & [\hat{Z}_{PV}] \\ [0] & [E] \end{bmatrix} \cdot \begin{bmatrix} [\overline{S}_d] & [0_1] \\ [0_2] & [V_d^2] \end{bmatrix} = \begin{bmatrix} [\overline{A}_{11}] & [\overline{A}_{12}] \\ [\overline{A}_{21}] & [\overline{A}_{22}] \end{bmatrix} \tag{13}$$

Where: $[\overline{A}_{11}] = [\hat{Z}_{PQ}] \cdot [\overline{S}_d]$, $[\overline{A}_{12}] = [\hat{Z}_{PV}] \cdot [V_d^2]$, $[\overline{A}_{21}] = [0]$, and $[\overline{A}_{22}] = [V_d^2]$.

$$[\overline{B}] = \begin{bmatrix} [\hat{Z}_{PQ}] & [\hat{Z}_{PV}] \\ [0] & [E] \end{bmatrix} \cdot \begin{bmatrix} [\hat{I}_{slack}] \\ [0_3] \end{bmatrix} = \begin{bmatrix} [\overline{B}_{PQ}] \\ [0_3] \end{bmatrix} \tag{14}$$

Where $[\overline{B}_{PQ}] = [\hat{Z}_{PQ}] \cdot [\hat{I}_{slack}]$.

Considering (13) and (14), (12) is rewritten as follows:

$$\begin{aligned} [\hat{U}] = \begin{bmatrix} [\hat{U}_{PQ}] \\ [\hat{U}_{PV}] \end{bmatrix} = \begin{bmatrix} [\overline{A}_{11}] & [\overline{A}_{12}] \\ [\overline{A}_{21}] & [\overline{A}_{22}] \end{bmatrix} \cdot \begin{bmatrix} [\overline{U}_{PQ}^{-1}] \\ [\overline{U}_{PV}^{-1}] \end{bmatrix} - \begin{bmatrix} [\overline{B}_{PQ}] \\ [0_3] \end{bmatrix} = \\ = [\overline{A}] \cdot [\overline{U}^{-1}] - [\overline{B}] \end{aligned} \tag{15}$$

From (15), the following formula is derived for calculating the conjugated node voltages:

$$\hat{U}_i = \sum_{k=1}^{N_{PQ}+N_{PV}} \frac{\bar{A}_{i,k}}{\bar{U}_k} - \bar{B}_i \,, i = 1 \ldots N_{PQ} + N_{PV} \tag{16}$$

Substituting (16) in (6) and (7) the following equations are obtained:

For PQ-nodes ($i = 1 \ldots N_{PQ}$):

$$\Delta\hat{S}_i = \left(\sum_{k=1}^{N_{PQ}+N_{PV}} \frac{\bar{A}_{i,k}}{\bar{U}_k} - \bar{B}_i \right) \sum_{k=1}^{N} \bar{Y}_{i,k} \bar{U}_k - \hat{S}_i = \\ = \hat{U}_i \bar{I}_i - \hat{S}_i = 0 \tag{17}$$

For PV-nodes ($i = N_{PQ} + 1 \ldots N_{PQ} + N_{PV}$):

$$\Delta P_{i-N_{PQ}} = \left(\sum_{k=1}^{N_{PQ}+N_{PV}} \frac{\bar{A}_{i,k}}{\bar{U}_k} - \bar{B}_i \right) \sum_{k=1}^{N} \bar{Y}_{i,k} \bar{U}_k + \\ + \bar{U}_i \left[\sum_{m=1}^{N_{PQ}+N_{PV}} \hat{Y}_{i,m} \left(\sum_{k=1}^{N_{PQ}+N_{PV}} \frac{\bar{A}_{m,k}}{\bar{U}_k} - \bar{B}_m \right) + \hat{Y}_{i,N} \hat{U}_N \right] - 2P_i = \\ = \hat{U}_i \bar{I}_i + \bar{U}_i \hat{I}_i - 2P_i = 0 \tag{18}$$

Where: $\bar{I}_i = \sum_{k=1}^{N} \bar{Y}_{i,k} \bar{U}_k$ and $\hat{I}_i = \sum_{m=1}^{N} \hat{Y}_{i,m} \hat{U}_m$.

The Jacobian matrix of the obtained system of nonlinear complex equations (17) and (18) is:

$$\left[\bar{J}\right] = \begin{bmatrix} \left[\frac{\partial \Delta\hat{S}}{\partial \bar{U}}\right] \\ \left[\frac{\partial \Delta P}{\partial \bar{U}}\right] \end{bmatrix} = \begin{bmatrix} \left[\bar{H}\right] \\ \left[\bar{L}\right] \end{bmatrix} \tag{19}$$

The elements of the Jacobian matrix are calculated with (20), (21) and (22).

$$\bar{H}_{i,j} = \frac{\partial \Delta\hat{S}_i}{\partial \bar{U}_j} = \bar{Y}_{i,j} \hat{U}_i - \frac{\bar{A}_{i,j}}{\bar{U}_j^2} \bar{I}_i \,. \tag{20}$$

Where: $i = 1 \ldots N_{PQ}$ and $j = 1 \ldots N_{PQ} + N_{PV}$.

$$\bar{L}_{i-N_{PQ},i-N_{PQ}} = \frac{\partial \Delta P_{i-N_{PQ}}}{\partial \bar{U}_i} = \bar{Y}_{i,i} \hat{U}_i - \frac{\bar{A}_{i,i}}{\bar{U}_i^2} \bar{I}_i - \\ - \frac{1}{\bar{U}_i} \sum_{k=1}^{N_{PQ}+N_{PV}} \hat{Y}_{i,k} \bar{A}_{k,i} + \hat{I}_i \tag{21}$$

Where $i = N_{PQ} + 1 \ldots N_{PQ} + N_{PV}$.

$$\bar{L}_{i-N_{PQ},j} = \frac{\partial \Delta P_{i-N_{PQ}}}{\partial \bar{U}_j} = \bar{Y}_{i,j} \hat{U}_i - \frac{\bar{U}_i}{\bar{U}_j^2} \sum_{k=1}^{N_{PQ}+N_{PV}} \hat{Y}_{i,k} \bar{A}_{k,j} \tag{22}$$

Where: $i = N_{PQ} + 1 \ldots N_{PQ} + N_{PV}$,

$j = 1 \ldots N_{PQ} + N_{PV}$,

and $j \neq i$.

Voltage corrections and new voltages at the k[th] iteration are calculated respectively with (23) and (24).

$$\left[\Delta\bar{U}\right] = -\left[\bar{J}\right]^{-1} \cdot \begin{bmatrix} \left[\Delta\hat{S}\right] \\ \left[\Delta P\right] \end{bmatrix} = -\begin{bmatrix} \left[\bar{H}\right] \\ \left[\bar{L}\right] \end{bmatrix}^{-1} \cdot \begin{bmatrix} \left[\Delta\hat{S}\right] \\ \left[\Delta P\right] \end{bmatrix} \tag{23}$$

$$\left[\bar{U}\right]^{(k)} = \left[\bar{U}\right]^{(k-1)} + \left[\Delta\bar{U}\right]^{(k)} \tag{24}$$

Modeling of FACTS devices is covered in [19] and [23].

2. LOADABILITY ASSESSMENT USING PARABOLA APPROXIMATION

a. Parabola Approximation Technique

Examining the imaginary part of the PV curve shown in Figure 2, it can be observed that beyond the loadability limit point this curve looks like a parabola. Therefore it is proposed here to approximate this curve with the following second-order polynomial:

$$P_1 = a_2 \cdot \left[imag\left(V_1\right)\right]^2 + a_1 \cdot \left[imag\left(V_1\right)\right] + a_0 \tag{25}$$

In order to determine the polynomial coefficients a_2 , a_1 and a_0 it is sufficient to have information on three points from the imaginary part of PV curve. This information can be obtained by performing three power flow computations in complex form, for three different P_1 beyond the loadability limit point. Then the polynomial coefficients are determined solving the following set of linear equations:

$$\begin{bmatrix} \left[imag(V_1^{(1)})\right]^2 & imag(V_1^{(1)}) & 1 \\ \left[imag(V_1^{(2)})\right]^2 & imag(V_1^{(2)}) & 1 \\ \left[imag(V_1^{(3)})\right]^2 & imag(V_1^{(3)}) & 1 \end{bmatrix} \cdot \begin{bmatrix} a_2 \\ a_1 \\ a_0 \end{bmatrix} = \begin{bmatrix} P_1^{(1)} \\ P_1^{(2)} \\ P_1^{(3)} \end{bmatrix} \tag{26}$$

Where the upper index enclosed by parentheses is the point number: 1, 2 and 3.

Actually, only a_0 is of interest here, so only this polynomial coefficient has to be calculated. It can be easily observed that the constant term a_0 of the approximation polynomial (25) corresponds to the limit power $P_{1,\lim}$, so generally $a_0 \approx P_{1,\lim}$. Thus, performing only three power-flow computations beyond the loadability limit point we can estimate the loadability limit.

b. Numerical results for a two-node system

The same two-node system as described in section III has been used here for exemplifying the above proposed parabola approximation technique. Numerical results for five loadability assessment case studies are presented in Table.

Table 1. Loadability assessment using parabola approximation : two-node system case study

Case no.	Point no.	Power flow results		Estimated $P_{1,lim}$, MW	Error, %
		P_1, MW	Imag(V_1), kV		
1	1	-70.4	1.9820	- 70.31848097515334	-3e-13
	2	-70.5	2.9575		
	3	-70.6	3.6832		
2	1	-71	5.7307	- 70.31848097515319	-6e-14
	2	-72	9.0016		
	3	-73	11.3674		
3	1	-71	5.7307	- 70.31848097515317	-2e-14
	2	-100	37.8192		
	3	-140	57.9466		
4	1	-85	26.5983	- 70.31848097515318	-4e-14
	2	-95	34.4870		
	3	-105	40.8807		
5	1	-140	57.9466	- 70.31848097451268	9e-10
	2	-141	58.3609		
	3	-142	58.7723		

Based on results presented in Table the following conclusions can be inferred for a two-node system:

1) The loadability limit determined using parabola approximation technique can be considered as one precisely calculated.

2) The accuracy of the loadability limit determined using parabola approximation approach practically does not depend on positions of those three points used for calculating the parabola coefficients.

3) Therefore, not only the imaginary part of PV curve looks like a parabola, but it is actually a parabola.

c. Numerical results for a multi-node system

The single-line diagram of a three-machine, nine-bus meshed system under consideration is shown in Figure 3. The power flow results are presented respectively in

Table and Table . All the values are in per unit on 100 MW base. The buses are numerated in the following order: first PQ-nodes, then PV-nodes, and finally the slack-bus.

The simulations have been carried out using Matlab software. A program has been written in Matlab to implement the power flow in complex form technique presented in section III.

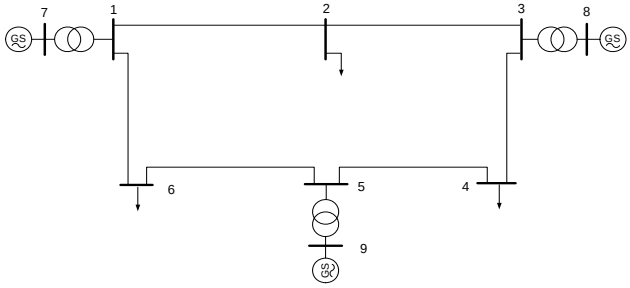

Figure 3. Three-machine, nine-bus meshed system
Transmission line data and bus data together with

Table 2. Transmission line data for the system in fig.3

From Bus Number	To Bus Number	Series Resistance R_s (pu)	Series Reactance X_s (pu)	Shunt Susceptance B/2 (pu)
7	1	0	0.0625	0
1	2	0.0085	0.072	0.0745
2	3	0.0119	0.1008	0.1045
3	8	0	0.0586	0
1	6	0.032	0.161	0.153
3	4	0.039	0.17	0.179
5	6	0.01	0.085	0.088
5	4	0.017	0.092	0.079
9	5	0	0.0576	0

Table 3. Bus data and power flow results for the system in Figure 3

Bus		Voltage		P_G (pu)	Q_G (pu)	P_L (pu)	Q_L (pu)
No.	Type	Magnit. (pu)	Angle (deg.)				
1	PQ	1.0258	3.7197	0	0	0	0
2	PQ	1.0159	0.7275	0	0	1.0	0.35
3	PQ	1.0324	1.9667	0	0	0	0
4	PQ	1.0127	-3.6874	0	0	0.9	0.3
5	PQ	1.0258	-2.2168	0	0	0	0
6	PQ	0.9956	-3.9888	0	0	1.25	0.5
7	PV	1.025	9.2800	1.63	0.0665	0	0
8	PV	1.025	4.6648	0.85	-0.1086	0	0
9	Slack	1.04	0	0.7164	0.2705	0	0

Node 2 has been chosen for loadability assessment. The system has been stressed by gradually increasing the load in node 2 (from 0 to 8 pu, in steps of 0.001 pu), while keeping the power factor constant. The lower part of PV curve has been built up by moving in the opposite direction (decreasing P_{L2}, from 8 to 0 pu). A series of power flow computations using the above mentioned program have been performed in order to build up the PV curve for node 2. The first power flow has been computed using flat start. The subsequent

power flow computations have been performed starting with the preceding power flow solution. The resulting PV curve is shown in Fig. 4.

The following conclusions can be drawn from Fig. 4:

1) The imaginary part of V_2 is zero for $P_{L2} \le P_{2,\lim}$ and is different from zero beyond the loadability limit point ($P_{L2} > P_{2,\lim}$).

2) Like in two-node system case, beyond the loadability limit point there are two complex conjugated solutions.

3) Therefore, the imaginary part of PV curve is symmetric about the P-axis and looks like a parabola.

4) Thus, the parabola approximation technique proposed above can also be applied to multi-node systems.

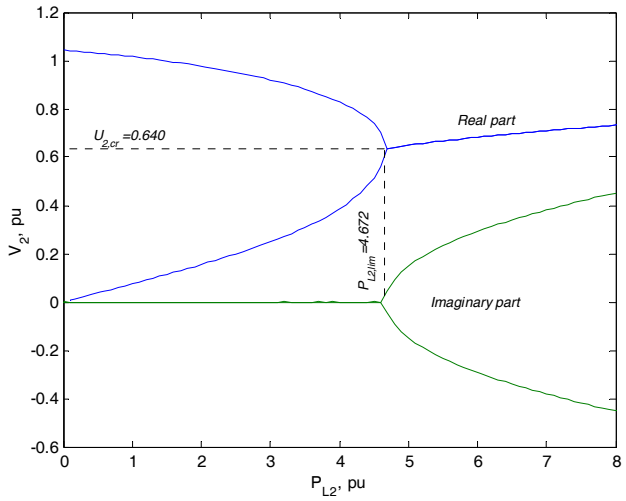

Fig. 4. PV curve for bus 2 of multi-node system

The parabola approximation technique has been applied to the multi-node system under consideration (shown in Figure 3) for estimating the loadability limit in node 2. Numerical results for seven loadability assessment case studies using parabola approximation technique are presented in Table 4.

Based on results presented in **Error! Not a valid bookmark self-reference.** the following conclusions can be inferred for a multi-node system:

1) The accuracy of the loadability limit determined using parabola approximation technique is quite satisfactory. The error is below 5%.

2) The accuracy slightly depends on positions of those three points used for calculating the parabola coefficients. A better precision is achieved when at least one point is situated close to the loadability limit point.

Table 4. Loadability assessment using parabola approximation: nine-node meshed system case study

Case no.	Point no.	Power flow results		Estimated $P_{L2,lim}$, pu	Estimation error, %
		P_{L2}, pu	*Imag*(V_2), pu		
1	1	4.68	0.0234	4.6725	-0.05
	2	4.69	0.0355		
	3	4.70	0.0444		
2	1	4.70	0.0444	4.6763	-0.14
	2	4.80	0.0947		
	3	4.90	0.1255		
3	1	4.70	0.0444	4.6978	-0.59
	2	6.40	0.3305		
	3	8.00	0.4518		
4	1	6.90	0.3731	4.7707	-2.16
	2	7.00	0.3810		
	3	7.10	0.3887		
5	1	7.90	0.4452	4.8199	-3.21
	2	8.00	0.4518		
	3	8.10	0.4582		
6	1	8.90	0.5065	4.8708	-4.30
	2	9.00	0.5121		
	3	9.10	0.5178		
7	1	5.00	0.1497	4.7431	-1.57
	2	7.00	0.3810		
	3	9.00	0.5121		

3) Thus, performing only three power flow computations in complex form, beyond the loadability limit point, we can estimate the loadability limit with an error below 5%.

4) In order to obtain a better accuracy, the same procedure has to be repeated. This time, the positions of those three points used for calculating the parabola coefficients are chosen close to the loadability limit obtained in previous step. Performing two steps of parabola approximation, the loadability limit can be determined very accurately (error below 0.5%).

3. SPARSITY, CONVERGENCE AND ILL-CONDITIONING ISSUES

a. Sparsity

It was mentioned earlier that an approach for solving the power flow equations in complex form has been previously reported in [17]-[19]. This method has the advantage that the sparsity of the Jacobian matrix is preserved, which is a key advantage in terms of computing time and memory storage in case of large power systems. This advantage is obvious when performing power flow computations up to the loadability limit point for large power systems. However, the method presented in [17]-[19] has also disadvantages. The problems with this method appear when performing power flow computations beyond the loadability limit point. In

this case, the computation time increases considerably due to the increased number of iterations. The number of iterations depends on initial voltage values imposed at the beginning of Newton-Raphson algorithm. Beyond the loadability limit point, it is very difficult to predict the initial voltage values that will ensure a small number of iterations, especially for large power systems. Therefore, it is practical to use the flat start, which results in an increased number of iterations with this method. Simulations show that the number of iterations increases up to 70 and more. Thus, although the computation time of a single iteration is reduced due to sparsity of the Jacobian matrix, the overall computation time increases considerably because of an increased number of iterations.

The method proposed in this paper does not have the above mentioned disadvantage. When performing power flow computations beyond the loadability limit point, using the method proposed in this paper and flat start, the convergence is ensured in 7-9 iterations. Although the computation time of a single iteration is increased, comparative with the method presented in [17]-[19], the overall computation time is reduced because of a small number of iterations.

As regards to memory storage requirements, nowadays, the computer memory is not an issue.

b. Convergence

Another significant disadvantage of the method presented in [17]-[19] is that it is prone to convergence towards unwanted solutions when performing power flow computations beyond the loadability limit point. This method is very sensitive to initial voltage values imposed at the beginning of Newton-Raphson algorithm. In order to direct this method to converge towards the appropriate solutions, the initial voltage values have to be chosen very carefully, that, in case of large power systems, is not a trivial issue and it is also time consuming. Otherwise, inappropriate solutions can be obtained, which are useless (cannot be used for loadability limit determination).

The power flow in complex form algorithm proposed in this paper reliably converges towards the appropriate solutions from flat start and there is no need in guessing the initial voltage values.

c. Ill-conditioning

Although the method proposed in this paper has the disadvantage that the sparsity (inherent in the original set of power flow equations) is destroyed, the Jacobian matrix is better conditioned, comparative with the method presented in [17]-[19]. This constitutes an advantage when performing power flow computations in proximity of the loadability limit point, where the Jacobian matrix is ill-conditioned, but also beyond the loadability limit point.

The problem of ill-conditioning usually appears in proximity of the loadability limit point. The loadability limit assessment approach proposed in this paper is based on complex power flow computations beyond the loadability limit point, where the Jacobian matrix is better conditioned than in its proximity. Numerous simulations have been carried out using the method proposed in this paper and no convergence problems have been encountered.

d. Comparative analysis

A comparative study has been performed, using the IEEE 300 Bus Power Flow Test Case [22] The simulations have been carried out on a Sony VGN-NW110D laptop using Matlab. In order the comparison to make sense, the method proposed in this paper and that presented in [17]-[19] have been tested under absolutely identical conditions. All the power flow computations have been performed using flat start. The solutions beyond the loadability limit point have been obtained by imposing a load of 9000 MW in node 1, all the other power flow data remaining unchanged. The simulation results are presented in Tabel 5.

Table 5. Comparative analysis: IEEE 300 bus power flow test case

Method	Presented in [17] – [19]		Proposed in the present paper	
Power flow condition	Up to the loadability limit point	Beyond the loadability limit point	Up to the loadability limit point	Beyond the loadability limit point
Computation time, seconds	1.8	15.8	5.3	11.5
Number of iterations	6	72	4	9
Condition number	1.0952×10^{5}	3.2262×10^{6}	7.4583×10^{4}	6.5723×10^{4}
Convergence	Converged to appropriate solutions	Converged to unwanted solutions	Converged to appropriate solutions	Converged to appropriate solutions

From Table 5, it can be seen that the method proposed in this paper has a better performance, comparative with the method presented in [17]-[19], when the power flow computations are carried out beyond the loadability limit point. To be mentioned

that the loadability limit assessment approach proposed in this paper is based on complex power flow computations beyond the loadability limit point. Using for this purpose the method presented in [17]-[19] can lead to erroneous results and increased computation time, due to drawbacks explained earlier.

4. NOMENCLATURE

$\overline{U}_i$, $\hat{U}_i$ – complex voltage at bus *i* and its conjugate*;

V_i – voltage magnitude at bus *i*;

$\overline{S}_i$, $\hat{S}_i$ – complex power at bus *i* and its conjugate;

P_i – active power at bus *i*;

$\overline{Y}_{i,j}$, $\hat{Y}_{i,j}$ – element from row *i* and column *j* of the bus admittance matrix and its conjugate.

* $\hat{U}_i$ is the conjugate of $\overline{U}_i$ only up to the loadability limit point. Beyond it, this does not hold true and $\hat{U}_i$ should be treated as an independent variable.

CONCLUSIONS

This paper proposes an approach for solving the power flow equations in complex form, i.e. without resorting to splitting each complex equation into two real equations. The conventional complex power flow equations are modified to meet the Cauchy-Riemann conditions and then are solved in complex numbers by applying the Newton-Raphson technique for complex variables (complex node voltages).

The proposed power flow in complex form converges beyond the loadability limit point, where the conventional power flow diverges. Although the solutions obtained beyond the loadability limit point are fictitious ones, they can be employed in loadability assessment. Beyond the loadability limit point, the node voltage magnitudes calculated with (5) are complex numbers, indicating that the power enforced in one or more nodes is above the loadability limit. Also, beyond the loadability limit point, the solutions obtained for node voltage magnitudes appear in complex conjugate pairs.

Since beyond the loadability limit point the node voltage magnitude is a complex number, the PV curve consists of two parts: real and imaginary (see Figure 2 and Fig. 4). Up to the loadability limit point, the imaginary part of PV curve is zero. Beyond the loadability limit point, the imaginary part of PV curve is different from zero and it looks like a parabola. Therefore, it is proposed to approximate the imaginary part of PV curve with a parabola. The constant term of the approximation polynomial corresponds to the limit power.

Using the parabola approximation approach proposed in this paper, the loadability limit can be determined after performing only three computations of power flow in complex form. Therefore, we find this technique suitable for online loadability assessment. The accuracy of the loadability limit determined using parabola approximation technique slightly depends on positions of those three points used for calculating the parabola coefficients, but it is quite satisfactory (typically the error is below 5%). The precision is higher when at least one point is situated close to the loadability limit point.

References

1. ***T. Van Cutsem, C. Vournas.*** *Voltage Stability of Electric Power Systems. Norwell: Kluwer Academic Publishers, 1998.*

2. ***C. W. Taylor****. Power System Voltage Stability (International Edition). New York: McGraw-Hill, 1994.*

3. ***P. Kundur.*** *Power System Stability and Control. New York: McGraw-Hill, 1994.*

4. ***C. A. Canizares, F. L. Alvarado***. *Point of collapse and continuation methods for large AC/DC systems, IEEE Trans. on Power Systems, vol. 8, no. 1, pp. 1-8, 1993.*

5. ***V. Ajjarapu, C. Christy.*** *The continuation power flow: a tool for steady stage voltage stability analysis, IEEE Trans. on Power Systems, vol. 7, no. 1, pp. 416-423, 1992.*

6. ***K. Iba, H. Suzuki, M. Egawa T. Watanabe***. *Calculation of critical loading condition with nose curve using homotopy continuation method, IEEE Trans. on Power Systems, vol. 6, no. 2, pp. 584-593, 1991.*

7. ***N. P. Patidar, J. Sharma,*** *Loadability margin estimation of power system using model trees, in Proc. of 2006 IEEE Power India Conf., New Delhi, India, 2006.*

8. ***G. D. Irisarri, X. Wang, J. Tong, S. Mokhtari****, Maximum loadability of power systems using interior point nonlinear optimization method," IEEE Trans.*

Power Systems, vol. 12, no. 1, pp. 162-172, Feb. 1997.

9. ***P. Acharjee, A. Indira, S. Mandal, S. S. Thakur***. *Maximum loadability limit of power systems using different particle swarm optimization techniques, in Proc. of IEEE Intern. Conf. on Industrial Engineering and Engineering Management (IEEM 2009), pp. 1573-1577.*

10. ***H. Sato***. *Computation of bifurcation and maximum loading limit in electrical power systems, in Proc. of the 2004 IEEE Intern. Conf. on Electric Utility Dereg., Restr. and Power Tech., Hong Kong, China, 2004, vol. 1, pp. 84-89.*

11. ***C. D. Vournas, M. Karystianos, N. G. Maratos***. *Bifurcation points and loadability limits as solutions of constrained optimization problems, in Proc. of IEEE Power Engineering Society 2000 Summer Meeting, vol. 3, 1883-1888.*

12. ***J. Kubokawa, H. Sasaki, S. Ahmed, G. Strbac***. *Application of optimal power flow for voltage stability problem, Proc. of Intern. Conf. on Electric Power Eng., Budapest, Hungary, 1999.*

13. ***X. Gu, C. A. Canizares.*** *Fast prediction of loadability margins using neural networks to approximate security boundaries of power systems, IET Gener., Transm. and Distrib., vol. 1, no. 3, pp. 466-475, 2007.*

14. ***A. Saffarian, B. Moradzadeh, M. Sanaye-pasand, S.H. Hosseinian***. *On-line prediction of closest loadability margins using neural networks, in Proc. of IEEE Region 10 Conference TENCON 2007, Taipei, Taiwan, 2007, pp. 1-4.*

15. ***S. Virmani, D. Vickovic, S.C. Savulescu***. *Real-time calculation of power system loadability limits, in Proc. of 2007 IEEE Lausanne Power Tech Conf., Lausanne, Zwitserland, 2007, 1278-1283.*

16. ***A. C. G. Melo, S. Granville, J. C. O. Mello, A. M. Oliveira, C. R. R. Domellas, J. O. Soto.*** *Assessment of maximum loadability in a probabilistic framework, in Proc. of IEEE Power Engineering Society 1999 Winter Meeting, vol. 1, 263-268.*

17. ***I. Axente***. *The Power Flow in Complex Form: A tool for steady-state stability analysis, Master's thesis, Dept. of Electric Power Eng., Royal Institute of Technology, Stockholm, 2002.*

18. ***I. Stratan, A. Cantar, and I. Axente***. *The mathematical model for calculation of operation regime using state equations in complex form, in Periodical on Electrotechnology, Power Engineering and Electronics "Buletinul Institutului Politehnic Iasi", Technical University Gh. Asahi, Iasi, Romania, 1999, vol. XLV (IL) FASC. 5, pp. 342-345.*

19. ***T. T. Nguyen and C. T. Vu***. *Complex-variable Newton-Raphson load-flow analysis with FACTS devices," in Proc. 2005/2006 IEEE Power Eng. Society Transm. and Distrib. Conf. and Exib., Dallas, Texas, USA, 2006, pp. 183-190.*

20. ***A. Gomez-Exposito, A. Conejo, and C. Canizares.*** *Electric energy systems: analysis and operation. New York: Taylor & Francis Group, 2009.*

21. ***R. V. Churchil.*** *Complex variables and applications. New York: McGraw-Hill, 1960.*

22. *The IEEE 300 Bus Power Flow Test Case. Available:*
http://www.ee.washington.edu/research/pstca/pf300/pg_tca300bus.htm

23. ***X. P. Zhang, C. Rehtanz, and B. Pal.*** *Flexible AC Transmission Systems: Modelling and Control. Berlin: Springer, 2006.*

24. ***S. Granville, J. C. O. Mello, A. C. G. Melo***. *Application of interior point methods to power flow unsolvability, IEEE Trans. Power Systems, vol. 11, no. 2, pp. 1096-1103, May 1996.*

Recommended for publication: 18.04.2012.